Applied Catalysis A: General 484 (2014) 154–160

Contents lists available at ScienceDirect

Applied Catalysis A: General

journal homepage: www.elsevier.com/locate/apcata

Biosynthesized ruthenium nanoparticles supported on carbon nanotubes as efficient catalysts for hydrogenation of benzene to cyclohexane: An eco-friendly and economical bioreduction method

Yao Ma, Yangqiang Huang, Youwei Cheng*, Lijun Wang, Xi Li

Department of Chemical and Biological Engineering, Zhejiang University, Hangzhou 310027, PR China

ARTICLE INFO

Article history:
Received 10 May 2014
Received in revised form 26 June 2014
Accepted 9 July 2014
Available online 17 July 2014

Keywords:
Biosynthesis
Ruthenium nanoparticles
Ruthenium catalysts
Benzene hydrogenation

ABSTRACT

Ru/carbon nanotubes (CNTs) catalysts synthesized by an environmentally benign and economical bioreduction approach were applied to the hydrogenation of benzene to cyclohexane under mild conditions without adding any solvent. The catalysts were characterized by a variety of techniques including BET, TEM, HAADF-STEM -EDX, XRD, XPS, FTIR, TG, and DTG. The effect of various preparation parameters, such as Ru loading, preparation temperature and calcination temperature on the catalytic performance were systematically analyzed and the optimum conditions were found to be 2 wt%, 60 °C, and 500 °C, respectively. In terms of reaction conditions, the combination of reaction temperature at 80 °C under the pressure of 4 MPa, and the time length of 0.5 h proved to be optimum, under which the cycohexane yield of 99.97% along with the TOF value of 6983.09 h^{-1} were achieved. Such results could match or even outweigh those reported in the literature. Furthermore, efforts were also made to probe the stability of catalysts. In a word, the merits of excellent durability, sound productivity and preferable reusability grant the catalysts a promising future in the industrial application.

1. Introduction

With the increasing industrial demands of low-aromatic diesel fuels, the development of effective catalysts for hydrogenation of arenes is of critical importance [1,2]. Poor fuel with high aromatic content produces a low cetane number in diesel fuel and a high smoke point in jet fuel. There is also evidence that particulate emissions in diesel exhaust gases correlate with the aromatic content in the fuel [2]. More and more stringent environmental laws and regulations have been enforced to bring down aromatics content to controllable level, which boosts new catalytic processes for aromatic saturation.

The hydrogenation of benzene to cyclohexane is one of the most important compounds hydrogenation reactions practiced in industry [3–5]. Cyclohexane is a valuable chemical used in the manufacture of nylon 6 and nylon 66, which constitute about 90% of all polyamides. In addition, cyclohexane is an excellent and nontoxic solvent for cellulose ether, wax, asphalt and rubber [6,7]. Nowadays, catalytic benzene hydrogenation to cyclohexane is the dominant production process in industry, although cyclohexane can be obtained from the separation of petroleum distillate [8]. There are lots of researchers [9,10] who use the catalytic benzene hydrogenation reaction to evaluate the performance of the hydrogenation catalysts. The use of homogeneous catalysts will inevitably encounter the separation problems which could be very sophisticated and money-consuming during the production process. Thus, to seek more economical heterogeneous catalysts becomes the primal concern for researchers in this field. The IFP process uses nickel-based heterogeneous catalysts at temperature above 200 °C under 50 bar [11,12]. These forcing conditions will lead to poor life-time performance, additionally, higher temperature will create favorable conditions for the side reactions such as isomerization and hydrocracking which result in selectivity of cyclohexane decline. Recently, several types of noble metals such as Ru, Rh, Pt, Pd, etc. have arose extensive interests and been used extensively as heterogeneous catalysts in the hydrogenation of benzene to cyclohexane [13–15]. In particular, considerable studies have focused on Ru-based catalysts which have extensively been investigated in hydrogenation processes. Nowicki et al. reported new colloidal solutions of Me-CD protected Ru(0) nanoparticles which were prepared by reduction of $RuCl_3$ with sodium borohydride [16]. They found these nanoheterogenous system present

* Corresponding author. Tel.: +86 571 8795 2210; fax: +86 571 8795 1227.
E-mail addresses: ywcheng@zju.edu.cn, uway@163.com (Y. Cheng).

http://dx.doi.org/10.1016/j.apcata.2014.07.015
0926-860X/

interesting activity for aromatic ring hydrogenation. Ozkar and coworkers prepared intrazeolite ruthenium(0) nanoclusters catalyst which exhibited excellent catalytic activity in the hydrogenation of benzene to cyclohexane [17].

The deposition-precipitation (DP) technique has long been used to synthesize Ru-based catalysts, which is not only energy intensive (because of numerous stringent conditions) but also hostile to environment (due to the use of toxic solvents or additives such as surfactant stabilizers and auxiliary capping agents). Compared to the conventional methods, bioreduction approach ("green chemistry") based on microorganisms or plants extract [18] is eco-friendly, cost-efficient and can be served as an alternative method to the DP technique to produce Ru nanoparticles. Biosynthesis of noble metal nanoparticles as an intersection of nanotechnology and biotechnology has gathered increasing interests in the last decade. Song and Kim reported the biosynthesis of Ag nanoparticles by using five plant leaf extracts (*Pine*, *Persimmon*, *Ginkgo*, *Magnolia* and *Platanus*) which could be used in various areas closely related with people's daily life such as cosmetics, foods and medical applications [19]. Zhan et al. successfully prepared Au nanoparticles by biogenic fabrication methods and they further immobilized the biosynthesized Au nanoparticles on TS-1 support which can act as bioreduction catalysts in vapor phase propylene epoxidation [20,21]. Although there are fewer attempts to apply the biosysthesized nanoparticles to catalytic system, it has been proved to be a promising approach for the fabrication of novel heterogeneous catalysts.

Owning to their unique properties and surfaces, Carbon nanotubes (CNTs) are suitable for many potential applications as promising carbon materials and solid supports for heterogeneous catalysts [22–25]. CNT-supported metallic nanoparticles exhibit remarkably high catalytic activities for hydrogenation of aromatic compounds. Pan and Wai developed a simple one-pot sonochemical method for the preparation of rhodium catalysts supported on CNTs which exhibited high catalytic activity of benzene and its derivatives hydrogenation without solvent under mild conditions [26]. Guo et al. reported Pt-based mono and bimetallic catalysts supported on CNTs by microwave-assisted polyol reduction method (MAPR) [27]. These catalysts were successfully applied to the selective hydrogenation of cinnamaldehyde to cinnamal alcohol. Effective dispersion of the nanocatalysts in organic solvents is one obvious reason favoring the CNT-supported metallic nanoparticles for catalytic hydrogenation reactions [25]. It becomes clear that, carbon nanotubes possess specific characteristics such as remarkable electronic properties, particular adsorption properties and high resistance to abrasion, all of which usher in a brighter prospect for such materials.

Hydrogenation of benzene to cyclohexane under mild conditions is also worthy of discussion from the perspective of energy and environmental considerations. In this paper, we probe into the biosynthesis of the Ru nanoparticles using the *Cacumen Platycladi* (*CP*) extract, which plays a dual role in reducing and protecting agent without any other additive and the immobilization of Ru nanoparticles on the nanoscale materials carbon nanotubes. The prepared catalysts were characterized by different techniques, including low temperature N_2 physisorption, transmission electron microscopy (TEM), high-angle annular dark field-scanning transmission electron microscopy (HAADF-STEM) with energy dispersive X-ray spectroscopy (EDX), X-ray diffraction (XRD), X-ray photoelectron spectroscopy (XPS), fourier transform infrared spectroscopy (FTIR), thermogravimetric (TG), and differential thermogravimetric (DTG). The performance of the bioreduction Ru-based CNTs catalysts was evaluated by the hydrogenation of benzene to cyclohexane without any solvents under mild conditions. In order to optimize the reaction parameters for maximum yield of cyclohexane and TOF value, the effect of various preparation and reaction conditions on the reaction was also included.

2. Experimental details

2.1. Materials

Carbon nanotubes (CNTs) were purchased from Bema Environmental Science and Technology Co. Ltd., *Cacumen Platycladi* (*CP*) was obtained from Zhejiang university hospital and other chemical reagents mentioned were analytic grade from Sinopharm Chemical Reagent Co. Ltd. and used directly without pretreatment.

2.2. Catalyst preparation

A series of Ru-based catalysts were prepared by the adsorption-reduction (AR) technique employing plant biomass extract [28]. Firstly, to obtain the *CP* leaf extract, screened powder *CP* leaf of 1 g dosage was dispersed in 100 mL deionized water under stirring for 4 h. The extract was then filtrated and used for the synthesis of RuNPs. In a typical catalyst preparation procedure, an appropriate amount of dried CNTs were immersed in aqueous $RuCl_3$ solution (50 mL, 2.2 mM) for 1 h in an oil bath (60 °C) under magnetic stirring. Afterward, 30 mL *CP* extract was added immediately into the mixture solution under stirring. After another 5 h, the products were filtered, washed thoroughly with deionized water, dried at 60 °C overnight in a vacuum oven, and then calcined at 500 °C for 3 h in the atmosphere of nitrogen. To investigate the influence of preparation parameters, different preparation conditions (Ru loading, 0.5–3.0 wt%; preparation temperature, 30–90 °C; calcination temperature, 200–700 °C) were implemented. To meet the needs of the characterization, the Ru nanoparticles (RuNPs) were prepared by reducing the metal precursor with the *CP* leaf extract free of the supports.

2.3. Catalyst characterization

Brunauer–Emmet–Teller (BET) specific surface areas were measured by N_2 adsorption at liquid N_2 temperature in an ASAP 2020 analyzer. Transmission electron microscopy (TEM), high-resolution transmission electron microscopy (HRTEM) and high-angle annular dark field-scanning transmission electron microscopy (HAADF-STEM) with energy dispersive X-ray spectroscopy (EDX) images were obtained with a FEI Tecnai G2 F20 S-TWIN microscope operated at 200 kV. The specimens were prepared by ultrasonically suspending the sample in ethanol for 0.5 h. Size distribution of the resulting NPs was estimated on the basis of TEM micrographs with the assistance of SigmaScan Pro software (SPSS Inc., Version 4.01.003). The X-ray diffraction (XRD) analyses were performed on a Shimadzu powder X-ray diffractometer with Cu Kα radiation at 40 kV and 30 mA using the scanning angle 2θ from 10° to 90°, at a step of 0.02° and rate of 2° min^{-1}. XPS experiments were performed on a VG ESCALAB MARK II equipment. Monochromatic radiation from an Mg Kα (BE = 1253.6 eV) X-ray source was used for excitation. FTIR spectra were recorded on a Nicolet 5700, where the samples were ground with KBr and pressed into the wafer. Thermogravimetric (TG) and differential thermogravimetric (DTG) analysis were measured with a METTLER TGA/SDTA 851^e thermobalance. The sample was heated from room temperature to 900 °C at a heating rate of 10 °C/min under a high purity nitrogen flow of 100 mL/min.

2.4. Catalyst evaluation

The hydrogenation of benzene to cyclohexane was carried out in a magnetically stirred 100 mL stainless steel high pressure

Table 1
Physical properties of synthesized catalysts.

	Sample	S_{BET} ($m^2\ g^{-1}$)[a]	V_p ($cm^3\ g^{-1}$)[b]	D_p (nm)[c]
1	Carbon nanotube	221	1.44	15.3
2	1.0% Ru/CNT[d]	216	1.05	16.0
3	1.5% Ru/CNT	204	1.13	17.7
4	2.0% Ru/CNT	194	0.93	18.6
5	2.5% Ru/CNT	177	1.00	18.4
6	3.0% Ru/CNT	176	0.92	19.7

[a] Specific surface area.
[b] Pore volume.
[c] Average pore diameter.
[d] Preparation conditions: preparation temperature 60 °C, calcination temperature 500 °C.

batch-type reactor. In a typical procedure, 3 mL neat benzene and 50 mg of the biosynthesized catalysts were placed in the reactor. The reactor was then sequentially sealed with flowing N_2 and H_2 at 4 MPa pressure to replace the air. Upon completion of the reaction, the reactor was quickly cooled in a water bath and depressurized with a connected pressure regulation. Liquid samples were centrifuged to separate the catalysts from the mixture. Gas chromatography (Ke Xiao, GC 1690) was used for the analysis of products of hydrogenation of benzene using N-hexane as the internal standard substance. The yield of cyclohexane and turnover frequency (TOF) value was calculated and used to evaluate the activity. TOF was calculated as moles of benzene consumed per surface of Ru site per hour. Repeated reaction runs with the same catalyst batch delivered yield/TOF values that were reproducible within ±2%.

3. Results and discussion

3.1. Characterization of the supports and catalysts

The nitrogen physisorption experiments conducted for the pure CNT and the Ru/CNT catalysts have shown their mesoporous structure. The physical properties of synthesized catalysts were presented in Table 1. The application of the unique structure of carbon nanotubes will significantly reduce mass transfer limitation which might be encountered in the micropores structure such as activated carbon [29]. Evidently, Table 1 indicated that the BET surface and the pore volume decreased slightly after the immobilization of the Ru nanoparticles into the channels of carbon nanotubes. As shown in Table 1, the BET surface plunged from 221 to 176 $m^2\ g^{-1}$ while the pore volume ranged from 1.44 to 0.92 $cm^3\ g^{-1}$ after Ru nanoparticles were introduced. Fig. 1 showed the N_2 adsorption/desorption isotherms and the pore size distributions for different Ru-based catalysts. Their adsorption isotherms were apparently classified as the types IV with an obvious hysteresis loop at the high P/P_0, according to BDDT classification, revealing typical mesoporous characteristics of the material [30]. As illustrated from the pore size distribution, the incorporation of the RuNPs led to the increase of the average pore diameters from 15.3 to 19.7 nm which was probably due to the extension role of the ruthenium nanoparticles [31].

The morphology and particle size of the bioreduction catalysts were studied by TEM. Fig. 2 represented the typical TEM images of the RuNPs and the size distribution. As illustrated, plenty of uniform nanoparticles showed a well-defined spherical shape and were distributed well on the carbon nanotubes. The high-resolution TEM image in Fig. 2d showed d-spacing of 2.06 Å, 2.14 Å and 2.34 Å, corresponding to (101), (002) and (100) facets of Ru respectively (ICDD-PDF-#65-7645) [32,33]. The histogram of their size distribution in Fig. 2b indicated that there exist nanoparticles measured between 1.5 and 5.5 nm and showed a relatively narrow size

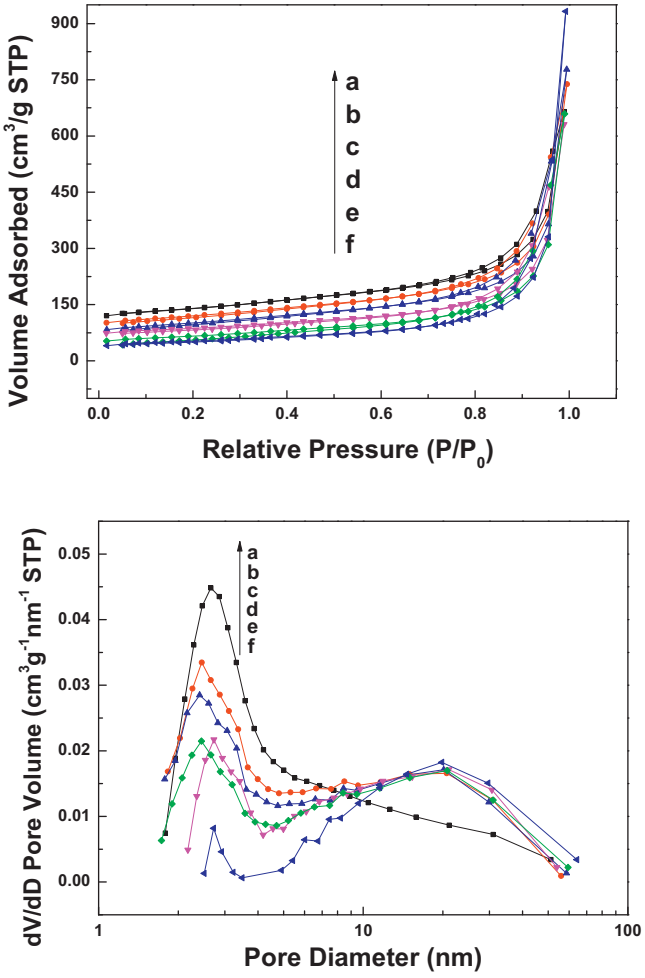

Fig. 1. Nitrogen adsorption–desorption isotherms and pore distributions isotherms for different catalysts varying Ru loading: (a) 0 wt%, (b) 1 wt%, (c) 1.5 wt%, (d) 2 wt%, (e) 2.5 wt%, and (f) 3 wt% (preparation conditions: preparation temperature 60 °C, calcination temperature 500 °C).

distribution of 3.06 ± 0.67 nm. Typical HAADF micrographs (Fig. 2e and f) confirmed the successful loading of the ruthenium nanoparticles. At different spots in the Ru/CNT catalyst, the presence of ruthenium, copper, molybdenum and carbon could be traced by the EDX while the Cu and Mo were introduced by the copper grid.

X-ray diffraction diagrams were recorded for a fresh CNT support, a calcined 2 wt% Ru/CNT, and an as-prepared RuNPs (Fig. S1 of Supplementary Information). The CNT sample showed the typical characteristic peaks at 2θ of 26.5° and 42.3°, indicating the existence of the hexagonal graphite structure. These peaks were identified by JCPDS-ICDD card: 65-6212 [34,35]. After incorporation of ruthenium in the graphite structure, there were no specific diffraction peaks of ruthenium in the XRD pattern of 2 wt% Ru/CNT. The catalysts preserved the main structure of the carbon nanotubes revealing the strong reflections of C structures (2θ = 42.3°), a low percentage of the ruthenium content and the high dispersion of the RuNPs on the support. In order to confirm the formation of Ru nanoparticles, they were prepared by reduction of the metal precursor with the *CP* leaf extract without introducing the supports and were characterized by the XRD analysis. Diffuse peaks were observed for a homogeneous distribution of quiet small Ru metal nanoparticles. All of the characteristic peaks of the metallic Ru were shown in the pattern. The diffraction angle of the peak at 44.1, 38.5, and 42.2, corresponding to the distance value (2.06 Å, 2.34 Å and

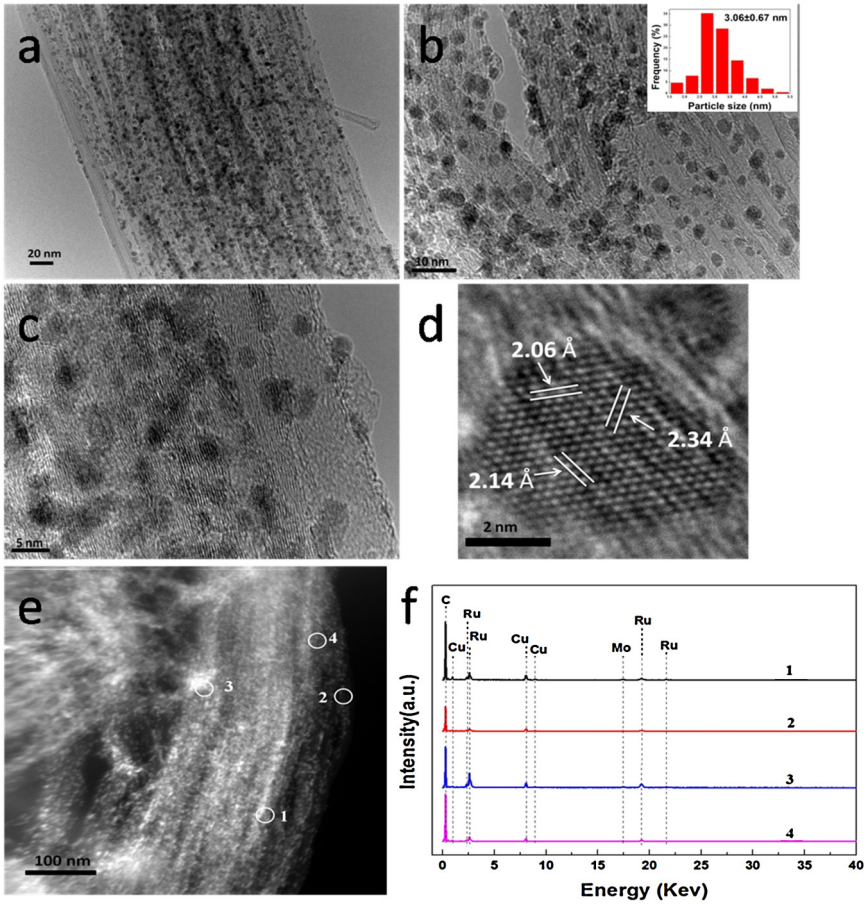

Fig. 2. Representative TEM images of Ru/CNT catalysts with different magnifications (a, b, and c). The inset in (b) indicates the size distribution of the ruthenium nanoparticles thereof. (d) A typical HRTEM micrograph of the Ru nanoparticles. (e) HAADF STEM images with specific spots and (f) the analysis of EDX (preparation conditions: Ru loading 2 wt%, preparation temperature 60 °C, calcination temperature 500 °C).

2.14 Å) were due to the (1 0 1), (1 0 0), and (0 0 2) plane of Ru metal (ICDD-PDF-#65-7645) respectively [32,33].

In order to establish the surface composition and chemical state of the bioredcution Ru nanoparticles, X-ray photoelectron spectroscopy (XPS) measurements were performed. The narrow scan spectra within the Ru 3d region (280–290 eV) showed highly overlapping Ru 3d and C 1s peaks (Fig. S2 of Supplementary Information). Since the C 1s experimental peak was too complicated to deconvolve, only a single contributing peak of 284.6 eV was applied for simplicity [36]. Out of our utmost interests, the peaks at 283.7 eV and 280.7 eV were assigned to Ru $3d_{3/2}$ and Ru $3d_{5/2}$ spin-orbit in the zerovalent state respectively. And the presence of Ru(IV) component probably resulted from air exposure during the XPS sample preparation [37]. During the reaction process under hydrogen atmosphere, the Ru nanoparticles were predominantly in the zerovalent state. The XPS measurements demonstrated the successful biosynthesis of Ru nanoparticles through a simple procedure of reducing $RuCl_3$ with *CP* extract.

FTIR analysis of the *CP* extract before and after bioreduction was carried out to identify the possible functional groups responsible for the reduction of ruthenium chloride and stabilization of the Ru nanoparticles. As shown in Fig. 3, the intensity of six bands at 3425, 2921, 1610, 1407, 1046 and 636 cm^{-1} was considerably attenuated after the bioreduction. The absorption bands at 2921 and 1610 cm^{-1} were associated with the stretching vibration of ν(=C–H) and ν(–C=C), respectively, while the band at 1407 cm^{-1} may be attributed to bending vibration of δ(O–H) [38]. Similarly, the band at 1046 cm^{-1} may be assigned to the stretching vibration of ν(–C–OH) [39]. Therefore, the functional groups of C=C–H or –C–OH in the plant extract were responsible for the reduction of ruthenium ions. Moreover, these functional groups could be adsorbed on the surface of the Ru nanoparticles to avoid agglomeration in which was similar to the mechanism of conventional stabilizer such as PVP [40]. To a large extent, these functional groups might be ascribed to polyols such as flavones and reducing sugars in the extract. From the results of FTIR analyses, the active

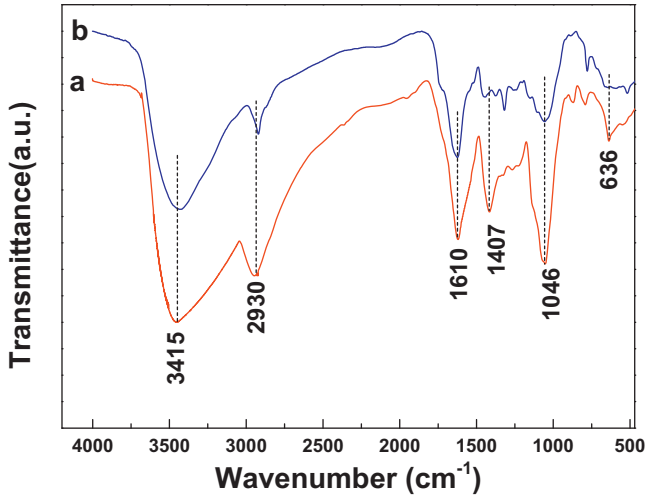

Fig. 3. Typical FTIR spectra of *Cacumen Platycladi* leaf extract before bioreduction (a), and after bioreduction (b) of ruthenium chloride.

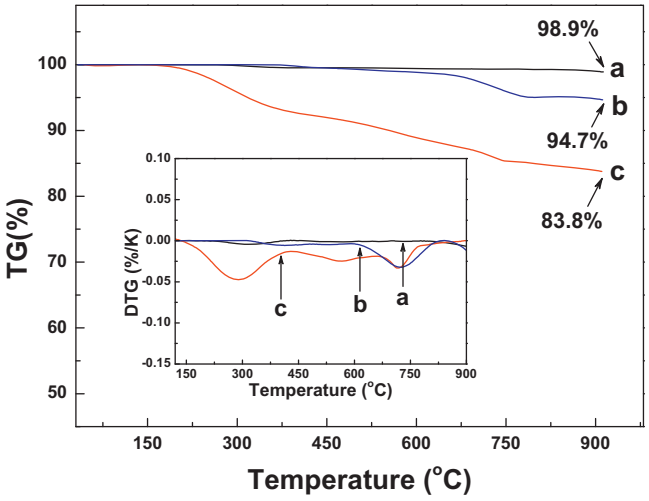

Fig. 4. TG and DTG profiles of (a) CNT support, (b) Ru/CNT catalyst with calcination temperature of 500 °C (preparation conditions: Ru loading 2 wt%, preparation temperature 60 °C), and (c) Ru/CNT catalyst without calcination (preparation conditions: Ru loading 2 wt%, preparation temperature 60 °C).

biomolecules responsible for the biosynthesis of the Ru nanoparticles might be flavones and reducing sugars.

The TG and DTG curves of CNT support, calcined Ru/CNT catalyst and uncalcined Ru/CNT catalyst were presented in Fig. 4. From the TG analysis, the presence of some plant biomass residual was confirmed. As shown in the picture, the plant biomass weighed 15.1% on uncalcined catalysts in contrast to only 4.2% on calcined catalysts. Actually, the amount of residual plant biomass was large when compared with other reported supports [28], demonstrating the superior adsorption property of the multiwalled carbon nanotubes. This plant biomass could act as the protective substances around the Ru nanoparticles. Results from the DTG analysis proved that the decomposition temperatures of the residual plant biomass were around 280 °C, 560 °C, and 730 °C. Although the plant biomass of the *Cacumen Platycladi* could prevent the metal nanoparticles from aggregation, we expected that proper calcinations treatment would contribute to the exposure of the active Ru surface. Hence, an appropriate calcination treatment was recommended following the results of TG and the evaluation parts.

3.2. Optimization of catalysts preparation conditions

3.2.1. Influence of Ru loading

The effects of Ru loading (0.5–3 wt%) on the catalytic activity of the bioreduction catalysts towards benzene hydrogenation were shown in Fig. 5. It is a well-known fact that various metal loading has remarkably different effects on the catalyst performance [41]. The Ru/CNT catalyst with the lowest Ru loading of 0.5 wt% presented a poor performance with only 21.32% the yield of cyclohexane and 1451.10 h^{-1} TOF value. The low metal loading along with the Ru active site insufficient might decrease the catalytic reactivity. Increasing the catalyst loading to 2 wt% gave rise to cyclohexane yield of 99.97% and TOF value of 6983.09 h^{-1}. However, too much load of Ru (Ru loading of 3 wt%) might result in loss of catalytic activity due to the larger particle size of the ruthenium nanoparticles. Consequently, the optimal Ru loading is 2 wt% at which the Ru active sites and the particle size were well balanced.

3.2.2. Influence of preparation temperature

The influence of the preparation temperature on the cyclohexane yield and the TOF value was investigated. The catalytic performance versus preparation temperature (30–90 °C) was

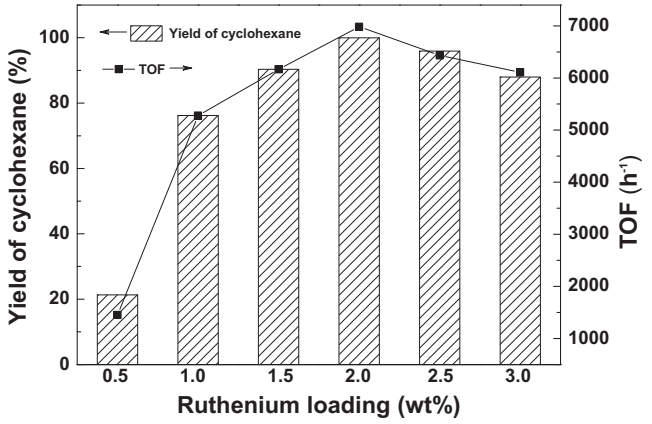

Fig. 5. Effect of Ru loading on the yield of cyclohexane and turnover frequency values (conditions: preparation temperature 60 °C, calcination temperature 500 °C, benzene 3 mL, catalyst 0.05 g, reaction temperature 80 °C, reaction pressure 4 MPa, reaction time 0.5 h).

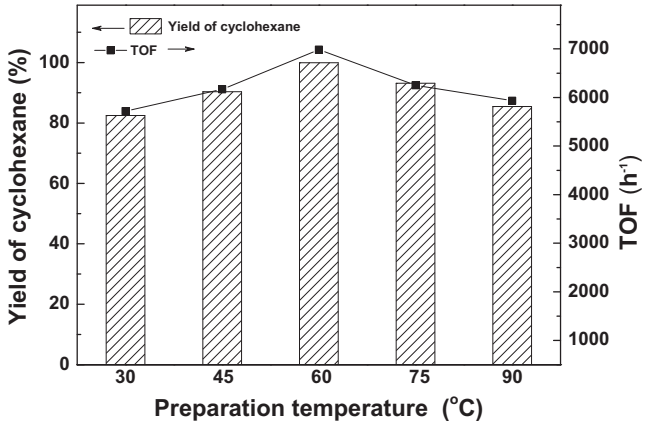

Fig. 6. Effect of preparation temperature on the yield of cyclohexane and turnover frequency values (conditions: Ru loading 2 wt%, calcination temperature 500 °C, benzene 3 mL, catalyst 0.05 g, reaction temperature 80 °C, reaction pressure 4 MPa, reaction time 0.5 h).

illustrated in Fig. 6. As shown, the preparation temperature was a sensitive factor which had an effect on the ultimate catalytic performance. When the preparation temperature was as low as 30 °C, the cyclohexane yield was 82.45% and the TOF value was 5718.84 h^{-1}. The cyclohexane yield and TOF value increased nearly linearly with the preparation temperature increasing. The yield of cyclohexane and the TOF value were 99.97% and 6983.09 h^{-1}, respectively, at the preparation temperature of 60 °C. The cyclohexane yield and TOF value oppositely decreased when preparation temperature of 60–90 °C is introduced. In general, the preparation temperature is corresponding with the reduction rate of the metal nanoparticles [42]. In our preparation system, the yield of cyclohexane and the TOF value first showed an upward trend and then a downward one. This led us to believe that 60 °C accompanied with a suitable reduction rate and homogeneous nucleation rate was a moderate preparation temperature that should be recommended.

3.2.3. Influence of calcination temperature

As shown in Fig. 7, the catalytic performance of benzene hydrogenation strongly depended on calcination temperature. As is known that calcination temperature plays an important role in the activation of the catalysts [43]. Appropriate calcination treatment could well balance between the ruthenium active sites exposed to the reactants and the stability of the Ru/CNTs catalysts, due to the prevention of Ru from agglomeration. Thus the conclusion drawn

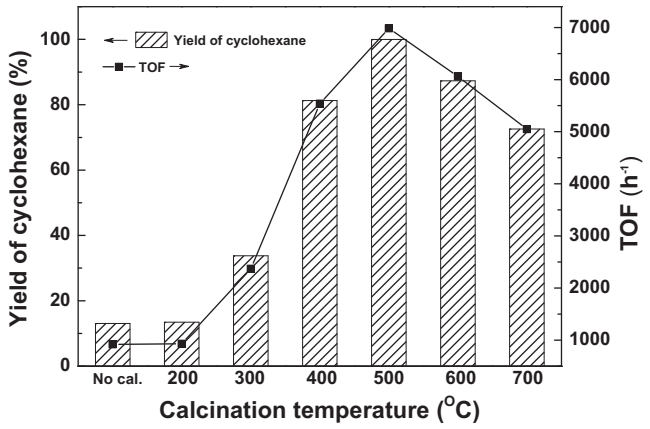

Fig. 7. Effect of calcination temperature on the yield of cyclohexane and turnover frequency values (conditions: Ru loading 2 wt%, preparation temperature 60 °C, benzene 3 mL, catalyst 0.05 g, reaction temperature 80 °C, reaction pressure 4 MPa, reaction time 0.5 h).

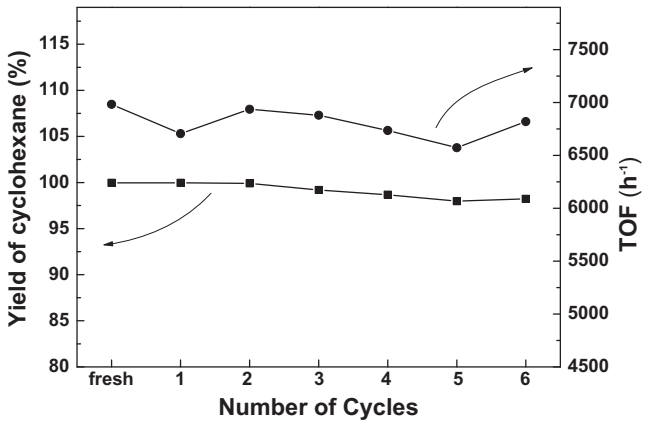

Fig. 8. The catalytic performance of recycling the bioreduced Ru catalyst (conditions: Ru loading 2 wt%, preparation temperature 60 °C, calcination temperature 500 °C, benzene 3 mL, catalyst 0.05 g, reaction temperature 80 °C, reaction pressure 4 MPa, reaction time 0.5 h).

from Fig. 7 showed that the catalysts without calcination were inert to catalytic activity which could be caused by the excessive plant biomass around the Ru nanoparticles. The data clearly indicated that the yield of cyclohexane increases steadily and continuously from 200 °C to 500 °C (from a low value of 13.45–99.97%). A suitable calcination of the catalysts would get rid of partial biomass (accounted for 9.9 wt% of the total catalyst weight according to the TG analyses) and made plenty of metal active sites exposed to the reactants. At the same time, the Ru/CNTs catalysts calcinated at 500 °C still contained 4.2% plant biomass according to the TG analyses. The yield of cyclohexane got the highest value of 99.97% when the calcination temperature was 500 °C, and it decreased to 72.56% as the calcination temperature increased to 700 °C. At this point, higher calcination temperature might remove most of the residual 4.2% plant biomass. It was this process that might lead to the agglomeration of the RuNPs. Hence, 500 °C was considered to be the optimum calcination temperature of the catalysts.

3.3. Durability of the bioreduction catalysts

The noble metal heterogeneous catalysts always suffer from rapid deactivation and the leaching problem [44,45]. In addition to the remarkable catalytic performance, the recyclability of the catalyst was also studied. The hydrogenation run was performed as described in Section 2.4. The catalysts after reaction were separated by centrifugation at a speed of 4000 rpm and the supernatant liquid was carefully removed by use of a syringe. The recycled catalyst was repeatedly washed by deionized water and ethanol. Fig. 8 illustrated the catalytic performance during six consecutive cycles and revealed that there was no significant decrease in the cyclohexane yield and the TOF value which indicated remarkable stability of the bioreduction Ru catalysts. The TEM analysis was introduced to elucidate the nature of the reused catalysts. As was seen from the pictures (Fig. S3 of Supplementary Information), the nanoparticles in the recycled catalysts remained at the

Table 2
The comparison of hydrogenation of benzene to cyclohexane catalyzed by Ru catalysts.

Catalyst	T (°C)[a]	P (MPa)[b]	t (h)[c]	Yield (%)[d]	TOF (h^{-1})[e]	Ref.
Ru/CNTs	80	4.00	0.5	99.97	6983	This work
Ru/C[f]				99.94	2747	
Ru/MMT	40	4.00	2.5	100	400	[46]
Ru/C[g]			5.0	99.50	200	
Ru/Al_2O_3[h]			3.5	35.60	102	
Ru/Methylated cyclodextrins	20	0.10	4.0	100	10	[16]
Ru/MOF[i]	60	6.00	2.0	>99	2475	[47]
Ru/MOF[j]			2.0	18	450	
Ru/C[k]			7.0	93	664	
Ru/PVPy	120	5.00	1.0	100	120	[37]
Ru/intrazeolite	22	0.28	2.0	90	1040	[14]
$Ru^{(0)}$/HAp	25	0.29	4.0	99	610	[48]
Ru/C composites[l]	25	3.00	2.0	100	50	[49]
Ru/CNT nanocomposites[m]	25	3.00	2.1	100	476	[50]

[a] Reaction temperature.
[b] Reaction pressure.
[c] Reaction time.
[d] Yield of cyclohexane.
[e] TOF was calculated as moles of benzene transformed per mole of active component per hour.
[f] The commercial 5% Ru/C catalyst from Aladdin Co. Ltd., China.
[g] From ICI CO., Japan.
[h] From XiAA Catal. Chem. Tech. Co. Ltd., China.
[i] The Ru/MOF catalyst synthesized in supercritical CO_2-methanol solution.
[j] The Ru/MOF catalyst synthesized in aqueous solution.
[k] The commercial Ru/C catalyst.
[l] The Ru/C catalyst synthesized by thermal decomposition from Ru acetylacetonate.
[m] The Ru/CNT catalyst synthesized in supercritical water.

identical state (3.12 ± 0.55 nm) and without obvious agglomeration. The excellent catalysts stability might be ascribed to the residue plant biomass (validated in the TG studies) as adhered to RuNPs, it could be served as a protecting agent and thus was able to prevent the leaching of the metal nanoparticles.

3.4. Comparison of the as-synthesized Ru-based catalyst with the existing catalysts

In order to test the exceptional catalytic activity of the bioreduction Ru/CNT catalyst synthesized under the optimal preparation conditions, varieties of hydrogenation reactions of benzene to cyclohexane under solventless circumstance at mild reaction condition were carried out. The most suitable reaction conditions were as follows: reaction temperature of 80 °C, reaction pressure of 4 MPa, and reaction time of 0.5 h. Under these mild conditions, 99.97% cyclohexane yield accompanied with quiet a high TOF value of 6983.09 h^{-1} was obtained. The yield of cyclohexane and the TOF value for benzene hydrogenation catalyzed by the bioreduction Ru catalysts, commercial reduced Ru/C and other Ru-based catalysts prepared by previously researchers were listed in Table 2. Obviously, the bioreduction catalysts, even with a lower Ru loading, could exhibit excellent catalytic activity when compared with the commercial Ru/C catalysts. It was clear that the as-synthesized Ru catalysts were very active for the hydrogenation of benzene to cyclohexane, with catalytic activity that was comparable or superior to other Ru-cluster-based catalysts. Higher cyclohexane yield, higher TOF value and milder reaction conditions could be simultaneously achieved in our catalytic system.

4. Conclusion

In summary, a novel and efficient method for the biosynthesis of Ru nanoparticles supported on carbon nanotubes was elucidated in this work. This eco-friendly catalyst had been successfully applied in the solventless hydrogenation of benzene to cyclohexane under mild conditions. The bioreduction nanoparticles with an average particle size of 3.06 nm showed a well-defined spherical shape and distributed well on the carbon nanotubes. In addition, the optimum operation conditions – Ru loading of 2 wt%, preparation temperature of 60 °C, calcination temperature of 500 °C, reaction temperature of 80 °C, pressure of 4 MPa, and the time length of 0.5 h were obtained. Under optimized conditions, the cycohexane yield of 99.97% along with the TOF value of 6983.09 h^{-1} were achieved, which was comparable or superior to other Ru-cluster-based catalysts. Moreover, the catalyst showed good recyclability for up to six runs consecutively without obvious agglomeration. The superior and stabilized catalytic performance makes this reaction system attractive for potential industrial applications.

Acknowledgments

This work was supported by the National Natural Science Foundation of China (No. U1361112) and the Fundamental Research Funds for the Central Universities (2013QNA4035).

Appendix A. Supplementary data

Supplementary data associated with this article can be found, in the online version, at http://dx.doi.org/10.1016/j.apcata.2014.07.015.

References

[1] A. Stanislaus, B.H. Cooper, Cat. Rev. Sci. Eng. 36 (1994) 75–123.
[2] B.H. Cooper, B.B. Donnis, Appl. Catal. A 137 (1996) 203–223.
[3] K. Weissermel, H.J. Arpe, Industrial Organic Chemistry, Fourth ed., 2003, pp. 313–336.
[4] J. Le Page, J. Cosyns, P. Courty, E. Freund, J. Franck, Y. Jacquin, B. Juguin, C. Marcilly, G. Martino, J. Miquel, Editions Technip, 1987, pp. 212.
[5] C. Vangelis, A. Bouriazos, S. Sotiriou, M. Samorski, B. Gutsche, G. Papadogianakis, J. Catal. 274 (2010) 21–28.
[6] J. Struijk, J. Scholten, Appl. Catal. A 82 (1992) 277–287.
[7] M. Saeys, M.-F. Reyniers, M. Neurock, G. Marin, J. Phys. Chem. B 109 (2005) 2064–2073.
[8] J. Garcia Villaluenga, A. Tabe-Mohammadi, J. Membr. Sci. 169 (2000) 159–174.
[9] L. Zhang, L. Wang, X.-Y. Ma, R.-X. Li, X.-J. Li, Catal. Commun. 8 (2007) 2238–2242.
[10] D. Durand, G. Hillion, C. Lassau, L. Sajus, US Patent 4 271 323 (1981).
[11] J.M. Larkin, J.H. Templeton, D.H. Champion, US Patent 5 189 233 (1993).
[12] M. Cessou, J. Cosyns, GB 1 313 084 (1104.1973) to Institut Franais du Ptrole.
[13] A.E. Coumans, D.G. Poduval, J. van Veen, E.J. Hensen, Appl. Catal. A 411 (2012) 51–59.
[14] S.K. Sharma, K.B. Sidhpuria, R.V. Jasra, J. Mol. Catal. A: Chem. 335 (2011) 65–70.
[15] C. Hubert, E.G. Bilé, A. Denicourt-Nowicki, A. Roucoux, Green Chem. 13 (2011) 1766–1771.
[16] A. Nowicki, Y. Zhang, B. Léger, J.-P. Rolland, H. Bricout, E. Monflier, A. Roucoux, Catal. Commun. 7 (2006) 296–298.
[17] M. Zahmakiran, S. Ozkar, Langmuir 24 (2008) 7065–7067.
[18] P. Mohanpuria, N.K. Rana, S.K. Yadav, J. Nanopart. Res. 10 (2008) 507–517.
[19] J.Y. Song, B.S. Kim, Bioprocess Biosyst. Eng. 32 (2009) 79–84.
[20] G. Zhan, J. Huang, L. Lin, W. Lin, K. Emmanuel, Q. Li, J. Nanopart. Res. 13 (2011) 4957–4968.
[21] G. Zhan, M. Du, D. Sun, J. Huang, X. Yang, Y. Ma, A.-R. Ibrahim, Q. Li, Ind. Eng. Chem. Res. 50 (2011) 9019–9026.
[22] S. Iijima, Nature 354 (1991) 56–58.
[23] S. Iijima, T. Ichihashi, Nature 363 (1993) 603–605.
[24] B. Yoon, C.M. Wai, J. Am. Chem. Soc. 127 (2005) 17174–17175.
[25] B. Yoon, H.-B. Pan, C.M. Wai, J. Phys. Chem. C 113 (2009) 1520–1525.
[26] H.-B. Pan, C.M. Wai, J. Phys. Chem. C 113 (2009) 19782–19788.
[27] Z. Guo, Y. Chen, L. Li, X. Wang, G.L. Haller, Y. Yang, J. Catal. 276 (2010) 314–326.
[28] G. Zhan, J. Huang, M. Du, D. Sun, I. Abdul-Rauf, W. Lin, Y. Hong, Q. Li, Chem. Eng. J. 187 (2012) 232–238.
[29] Y. Huang, Y. Ma, Y. Cheng, L. Wang, X. Li, Ind. Eng. Chem. Res. 53 (2014) 4604–4613.
[30] S. Brunauer, L.S. Deming, W.E. Deming, E. Teller, J. Am. Chem. Soc. 62 (1940) 1723–1732.
[31] M. Du, G. Zhan, X. Yang, H. Wang, W. Lin, Y. Zhou, J. Zhu, L. Lin, J. Huang, D. Sun, J. Catal. 283 (2011) 192–201.
[32] A.M. Karim, V. Prasad, G. Mpourmpakis, W.W. Lonergan, A.I. Frenkel, J.G. Chen, D.G. Vlachos, J. Am. Chem. Soc. 131 (2009) 12230–12239.
[33] X. Ni, B. Zhang, C. Li, M. Pang, D. Su, C.T. Williams, C. Liang, Catal. Commun. 24 (2012) 65–69.
[34] G. Ovejero, J. Sotelo, A. Rodriguez, C. Diaz, R. Sanz, J. Garcia, Ind. Eng. Chem. Res. 46 (2007) 6449–6455.
[35] J.A. Rajesh, A. Pandurangan, Chem. Eng. J. 243 (2014) 436–447.
[36] C.D. Wagner, Physical Electronics Division, Perkin-Elmer Corp., 1979.
[37] M. Fang, N. Machalaba, R.A. Sánchez-Delgado, Dalton Trans. 40 (2011) 10621–10632.
[38] D. Williams, I. Fleming, Spectroscopic Methods in Organic Chemistry, 1980, pp. 35–73.
[39] H. Chen, J. Wang, D. Huang, X. Chen, J. Zhu, D. Sun, J. Huang, Q. Li, Mater. Lett. 122 (2014) 166–169.
[40] X. Yang, Q. Li, H. Wang, J. Huang, L. Lin, W. Wang, D. Sun, Y. Su, J. Opiyo, L. Hong, Y. Wang, N. He, L. Jia, J. Nanopart. Res. 12 (2010) 1589–1598.
[41] J. Huang, C. Liu, D. Sun, Y. Hong, M. Du, T. Odoom-Wubah, W. Fang, Q. Li, Chem. Eng. J. 235 (2014) 215–223.
[42] J. Huang, G. Zhan, B. Zheng, D. Sun, F. Lu, Y. Lin, H. Chen, Z. Zheng, Y. Zheng, Q. Li, Ind. Eng. Chem. Res. 50 (2011) 9095–9106.
[43] L. Wang, J. Chen, L. Ge, V. Rudolph, Z. Zhu, J. Phys. Chem. C 117 (2013) 4141–4151.
[44] M. Lamblin, L. Nassar-Hardy, J.C. Hierso, E. Fouquet, F.X. Felpin, Adv. Synth. Catal. 352 (2010) 33–79.
[45] R. Kouraichi, J. Delgado, J. López-Castro, M. Stitou, J. Rodríguez-Izquierdo, M. Cauqui, Catal. Today 154 (2010) 195–201.
[46] S. Miao, Z. Liu, B. Han, J. Huang, Z. Sun, J. Zhang, T. Jiang, Angew. Chem. Int. Ed. 45 (2006) 266–269.
[47] Y. Zhao, J. Zhang, J. Song, J. Li, J. Liu, T. Wu, P. Zhang, B. Han, Green Chem. 13 (2011) 2078–2082.
[48] M. Zahmakıran, Y. Tonbul, S. Özkar, Chem. Commun. 46 (2010) 4788–4790.
[49] J. Calderon-Moreno, V. Pol, M. Popa, Eur. J. Inorg. Chem. 18 (2011) 2856–2862.
[50] Z. Sun, Z. Liu, B. Han, Y. Wang, J. Du, Z. Xie, G. Han, Adv. Mater. 17 (2005) 928–932.